

Referee 1

English is of poor quality. I sure the text should be subjected to the thorough English language edition either by professional English editor or by colleague fluently speaking English.

The English was edited.

All your correction are considered and added.

New references added

Referee 2

The paper is a poor in several aspects.

First of all the English, even if understandable, is vary bad, with sentences without the verb, full stops inserted without a reason, repeated words and misprints even in the references (Carrazzo MT is indeed Carrozzo MT, Negra S is indeed Negri S).

The English was edited and modified to be understaned.

All the grammar correction and spelling are corrected

That said, I don't see either some deep discussion about the performed processing or a discussion an adequate discussion about the archaeological interpretation of the identified remains.

We tried to modify the discussion.

I would also drop out the part about the technique of the GPR. It is clear that this is not the area of expertise of the authors and there are books or papers that could referred to this pros.

We drop all parts about the technique of the GPR.

If there will be a substantial revision of the grammar and fluency, and something more consistent about either the processing and/or the archaeological interpretation of the results.

The grammar reviewed, more consistent about interpretation of the results added.

1 **Ground-penetrating radar inspection of Subsurface Historical Structures at the**
2 **Baptism (El-Maghtas) site, Jordan**

3
4 ⁽¹⁾AbdEl-Rahman Abueladas* , ⁽¹⁾Emad Akawwi

5
6 ⁽¹⁾Surveying and Geomatics Department, Faculty of Engineering, Al-Balqa Applied
7 University, Al-Salt 19117, Jordan.

8
9 * Corresponding author e-mail: aabueladas@bau.edu.jo, Tel: +962 0791709827,
10 Fax: +962 5 3530465

11 **Abstract**

12 The Baptism (El-Maghtas) site is located to the north of the Dead Sea on the eastern bank
13 of the Jordan River. Previous archeological excavations in the surrounding area have
14 uncovered artifacts that include the location was home to "John the Baptist," who lived
15 and preached in the early 1st Century AD and is known for baptizing Jesus. Archeological
16 excavations have revealed walls, antiquities, and ancient water systems that include
17 conduits, pools, and ancient pottery pipes. A Ground Penetrating Radar (GPR) survey
18 was carried out at select locations along parallel profiles using a Subsurface Interface
19 Radar System (Geophysical Survey Systems Inc. SIRvoyer-20) with 400 MHz or 900
20 MHz mono-static shielded antennas in order to locate archaeological materials at shallow
21 depths. The GPR profiles revealed multiple subsurface anomalies across the study area.
22 At the John the Baptist Church site buried wall were detected along the profiles, and at
23 the pool site the survey delineated several buried channels. GPR data also confirmed the
24 extension of an ancient pottery pipe at Elijah's Hill site through the production of a clear
25 diffraction hyperbola anomaly related to the ancient pottery pipe that could be
26 discriminated from the 2D profiles. The GPR data was displaced using 3D imaging to
27 define the horizontal and vertical extent of the pipe.

28
29 *Keywords:* Jordan River, Baptism, Archaeological remains, pottery pipe, Ground
30 Penetrating Radar.

31
32
33
34
35
36
37
38
39
40
41
42
43
44
45
46

47 **1 Introduction**

48 Locating an archeological site that contains buried artifact, and antiquities has
49 traditionally methods such as coring, foretelling, and shovel testing, which are time-
50 consuming and labor intensive procedures that can lead to significant waste of time and
51 expense. Ground-penetrating radar (GPR) is a unique high-resolution tool that offers a
52 solution to these problems (Vaughan 1986).

53 GPR uses electromagnetic (EM) waves with frequencies of 10-1000 MHz to picture
54 subsurface soil and structure. It has become an accepted method for use in various fields,
55 including archaeology, geology, engineering and construction, environmental fields, and
56 forensic science (Neal 2004). The advantage of using EM waves with relatively short
57 wavelengths lies in the ability to map small objects at shallow depth. This GPS
58 methodology has been successfully utilized to locate antiquities in urban and arid settings
59 (Vaughan 1986; Sternberg and McGill 1995; Cacione et al. 1996; Basile et al. 2000,
60 Ronen et al., 2018) and has proven to be an efficient method for identifying areas with
61 the highest potential for successful excavation (Cacione 1996).

62 Additionally, GPR data presentations can play a significant role in archaeological
63 inspections since they provide a visual representation of the site, including the size and
64 depth of any subsurface anomalies (Basile et al. 2000).

65 The main objective of this study to carry out a ground-penetrating radar (GPR) survey,
66 which is a non destructive and non-invasive method of obtaining information about the
67 existence of archaeological features in shallow subsoil and to image the extension of a
68 partially excavated ancient pottery pipe. The Baptism Site is situated approximately eight

69 kilometers from the northern corner of the Dead Sea on the eastern bank of the Jordan
70 River (Fig. 1).

71 Figure 1

72 The site is located in an arid environment where a large number of archaeological
73 remains of various age, and size are located in variable geological–archaeological media
74 (Eppelbaum et al., 2010). Soils at the site are complex, and in some locations vegetation
75 factors complicate the accessibility of GPR survey (Eppelbaum and Khesin, 2001;
76 Eppelbaum et al., 2010).

77 The GPR survey was carried out at three different sites to identify any shallow anomalies

78 **2 Historical Background**

79 The Baptism (El-Maghtas) site is a prehistoric area in Jordan Valley, about 50 km from
80 Amman in western Jordan, settlements within El-Maghtas known as Bethany in the place
81 where John the Baptist lived in the time of Christ, making El-Maghtas one of the most
82 important archaeological sites associated with early Christianity.

83 John the Baptist's settlement is connected with several biblical events including the
84 baptism of Jesus which took place in Bethany, Joshua's crossing of the Jordan River, the
85 last days of Moss, and the Prophet Elijah's crossing of Jordan where he ascended to
86 heaven in a whirlwind upon a chariot with horses of fire (2 Kings 2:5-14). For nearly
87 2000 years, local church traditions and pilgrimages have identified the small hill at the
88 center of Bethany as the site from which Elijah was raised to paradise. The site became
89 famous for this hill, Elijah's Hill (also Tell Mar Elias, Jabal Mar Elias), which is located
90 2km west of the Jordan River

91 The settlement of Bethany and surrounding regions in Jordan has been known by various
92 names throughout history including Ainon, Saphaphas, Bethanin, and Bethabra (Beit el-
93 Obour, or house of the crossing), Arabic language bibles refer to it as Beit' Anya. Thus,
94 today the entire region that falls between Bethany and the Jordan River is called El-
95 Maghtas (the place of immersion or baptism).

96 Current archaeological studies in the area have identified numerous structures, including
97 monastic complexes, churches, caves, and a system of water pipes, and channels as well
98 as other facilities from the Roman and Byzantine era (4th to 8th centuries AD) (Waheeb
99 2001). Effectively, these excavations have revealed a settlement from the time of Jesus
100 and John the Baptist (early 1st century AD).

101 The existence of excavated water structures, such as aqueducts, pools, cisterns, and
102 pottery pipes, attests to the complexity of the water system in the area. Previously settlers
103 had depended on rainwater catchments and springs as a sources of water, prompting the
104 Roman and Byzantine to divert water from nearby Wadi using conduit and pottery pipes
105 to fill pools and cisterns as reservoirs (Waheeb 2003).

106 **3 GPR concepts**

107 Ground-penetrating radar (GPR) is a high-resolution method of picturing subsurface
108 structures using electromagnetic (EM) waves with a frequency band from 10 MHz to 1
109 GHz. The benefit of using (EM) waves is that signals of a relatively short wavelength that
110 can be generated and directed to the subsurface to map anomalous vary in their electrical
111 properties, in many aspects.

112 The horizontal resolution links to the ability to detect reflector location in space or time,
113 which is a function of the pulse width. The vertical resolution increases with an increase

114 in the frequency. The vertical resolution is also controlled by wavelength (λ) (Knapp,
115 1990), which is a function of velocity and frequency:

$$116 \quad \lambda = v/f$$

117 The best vertical resolution can be obtained by using one-quarter of the dominant
118 wavelength (Sheriff 1977).

119 **4 GPR Survey**

120 A continuous GPR survey was conducted utilizing an SIRvoyer-20, produced by
121 Geophysical Survey Systems, Inc. (GSSI). 900 MHz and 400 MHz frequency antennas
122 were used in this study. A total of 88 meters of GPR surveys were conducted along 11
123 profiles at three different sites. The first survey site is located to the north of John the
124 Baptist Church, the second to the south of the pools, and the third at Elijah's Hill.

125 Three profiles were conducted at each of the first two sites and five additional profiles
126 were carried out on the south side of at the last site Elijah's Hill (Fig. 1). At the second
127 and third sites, the surveys used a 900 MHz antenna.

128 **4.1 Data processing**

129 Minimum data processing was applied to utilize the GSSI RADAN V software package
130 from GSSI. Horizontal and vertical high and low pass filters have been applied to
131 enhance the radar cross-section and to eliminate the surplus noise from the GPR signal.
132 Additional processing to convert two-way travel times along the section to depth in meter
133 applying average radar wave velocity. Data were stacked in the horizontal direction along
134 with profiles. The Data then edited while both horizontal and vertical scales were attuned
135 before processing (Abueladas, 2005).

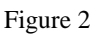
136 Time-zero correction was applied to the raw GPR data, which were then managed
137 using range and display gain, filtering, color conversion, and migration procedures
138 (Aqeel et al. .2014).

139 The obtained GPR data were processed and presented as 2-D depth cross-sections
140 providing a logical vertical/horizontal resolution for the upper 2 m of the inspected sites
141 (Odah et al., 2013). Calculation of the subsurface radar-wave velocity is essential to
142 [convert the two way travel time \(TWT\)](#) of the reflected signal to the real depth of the
143 reflector (Annan 2003; Fisher et al. 1992). However, this study calibrated the velocity
144 according to the known depth aligned with the top of the excavated pipe near the study
145 area.

146 The dielectric permittivity of the various areas is obtained using an approximation of the
147 reflection delay formula, which connects wave velocity (v), to measured depth (x), the
148 recorded two-way travel time (t), the relative permittivity (ϵ_r), and the free-space velocity
149 (c) (Gracia et al. 2008)

150
$$\epsilon_r = \left(\frac{c}{v}\right)^2 = \left(\frac{ct}{2x}\right)^2$$

151 The computed near-surface average velocity was 0.12 m/ns (Fig. 2).

152 

153 **5 Results and discussion**

154 [Because the lack of geophysical and archaeological data for the study area, therefore it](#)
155 [was too difficult to interpret the GPR data.](#)

156 A total of three continuous parallel profiles up to 12 m long were recorded at site number
157 The separation between the adjacent west-east profiles is constant at 1 m (Fig. 1).

158 The 400 MHz antenna radar gram along profile 4001 shows a large discontinuous linear
159 discontinuous anomaly at approximate depth of 1.2 m, that is interpreted as a
160 discontinuous buried wall and can be viewed in figure 3.

161 Figure 3

162 Profile 4002, which is located 1m to the north, shows the same anomaly that was
163 observed in profile 4001, however it was detected at shallower depth (Fig. 4).

164 These anomalies are caused by dissimilarities in wave velocity at the point of contact
165 between disparate materials. Their depths and extensions of these anomalies most likely
166 indicate the possibility that buried wall with a north-south orientation is presented in
167 subsurface. No other anomalies were detected within profile 4003.

168 Figure-4

169 At site 2 and 3 a 900 MHz antenna with good spatial resolution was used and repeated
170 GPR survey was performed along the profiles to provide more information about
171 subsurface structures.

172 A 900 MHz antenna survey was conducted at site 2 along profile 9001 from west to east
173 (Fig. 1). Figure 5 shows one primary anomaly at a depth of 0.25 m, located between the 1
174 m and 3m markers that is interpreted as a buried wall. The 3-meter-wide depression at the
175 end of the profile may be correlated to a shallow buried channel.

176 Figure-5

177 Profile 9002 is 10 m long and runs parallel to profile 9001, approximately 1 m to the
178 north (Fig. 1). The same anomaly and depression were detected along this profile as were
179 found in profile 9001 (Fig. 6).

180 Figure-6

181 The 12 m long profile 9003 is located to the north of profile 9002 closer to the pool (Fig.
182 1). The radar profile shows an anomaly between the 2 m and 5 m markers at an
183 approximate depth of 0.25 m, which is interpreted as a buried wall (Fig. 7). The bottom
184 of the depression along this profile is deeper, and the width is lesser than profiles to the
185 south.

186 Figure-7

187 Site 3 is a 2 by 5 m a rectangular section on a flat area near Elijah's Hill. The uni-
188 directional survey was conducted along five profiles oriented approximately north-south
189 and spaced 0.5 m apart to the east of the excavated section of pottery pipe (Fig. 1).

190 The pottery pipe is one of the structures associated with an ancient water system. Most
191 sections of this pipe were destroyed by human activities, but an intact segment was
192 successfully excavated within the site.

193 GPR profile 1 was collected perpendicular to the trend of the excavated pottery pipe just
194 east of the excavation using a 900 MHz antenna (Fig. 1). The hyperbolic-shaped anomaly
195 appears at the 2.5 m mark, and is about 0.55 m deep showing the location of the buried
196 pipe (Fig. 8).

197 Figure-8

198 The main anomalies appear as diffraction hyperbolas with high amplitudes, observed at
199 the 2.5 m marker and at 0.55 m depth, along the entirety of the 2D ground-penetrating
200 radar cross-section.

201 Generally, targets of interest are easier to identify using three-dimensional data rather
202 than conventional two-dimensional profile lines. The 3D GPR data were generated from

203 2D and displayed using 3D-visualisation techniques, which is of primary importance in
204 archaeological applications.

205 A 3D perspective view of the processed profiles using high pass and low pass vertical
206 and horizontal filters together with the migration technique illustrates the location of the
207 pottery pipe (Fig. 9) (Whiting 2001; Fisher et al. 1992a).

208 **Figure-9**

209 Depth slices [which are useful for accurate interpretation were generated](#) at different
210 depths (0, 0.25, 0.55, 0.75 m) from the 3D plot are presented in figure 10. The main
211 anomaly observed on the depth slice of 0.55 mbs (meter below the surface) has a west-
212 east orientation and corresponds to the pottery pipe anomaly, which provide good
213 information about the exact location and extension of the pipe.

214 **Figure-10**

215 The multiple slices view along the y-direction at various distances (0, 1, and 2 m)
216 determines the extension of the pipe anomaly along the y-direction (Fig. 11).

217 **Figure-11**

218 The 3D section (chair view) with $X= 2.5$ m, $Y= 0.85$ m, and $Z= 0.55$ m shows clearly the
219 east-west extension of the pipe perpendicular to the X position, and the depth to the top
220 of the pipe determined by the Z position (Fig. 12). The results of this study showed that
221 many subsurface structures were recognized using GPR. Subsurface walls were
222 delineated and various subsurface channels were found.

223 **Figure-12**

224 The locations of these channels were well defined and flow directions in these channels
225 were also identified from west to east in the study area. Fig. 13 shows the location map of
226 GPR anomalies and their interpretation.

227  Figure-13

228 **6 Conclusions**

229 Ground-penetrating radar (GPR) is a powerful, non-destructive, non-invasive geophysical
230 near-surface tool for archaeological surveying. GPR has been used successfully in this
231 study to detect several shallow anomalies at El-Maghtas Site. The flat topography and the
232 absence of archaeological features at the surface of the site allowed for collection of
233 good quality GPR data. The high frequency 900 MHz antenna was used successfully to
234 locate smaller archaeological objects at shallow depths and 3D images provided high
235 resolution than the 2D profiles, as can be seen from the results. Generally, the survey
236 included the identification and mapping of covered walls, channels, and the extension of
237 an ancient pottery pipe.

238 However, vertical sections, depth slices, and 3D images were used to locate the
239 anomalies using spatial extent 3D survey, allowing for a precise detection of the anomaly
240 throughout the surveyed data after advanced processing, including migration. Using
241 three-dimensional GPR imaging allowed for the successful detection of the east-west
242 oriented extension of the pottery pipe in the El-Maghtas Site.

243 *The mapped archaeological targets are relatively shallow, showing detectable anomalies
244 from approximately 0.55 m below the ground surface extending to a depth of 1.2 m.*

245 The displacement shown in the buried wall and channel in site 2 may be caused by a
246 shallow fault. *The results of this study can be used as a source for any future excavations.*

247 **Acknowledgments**

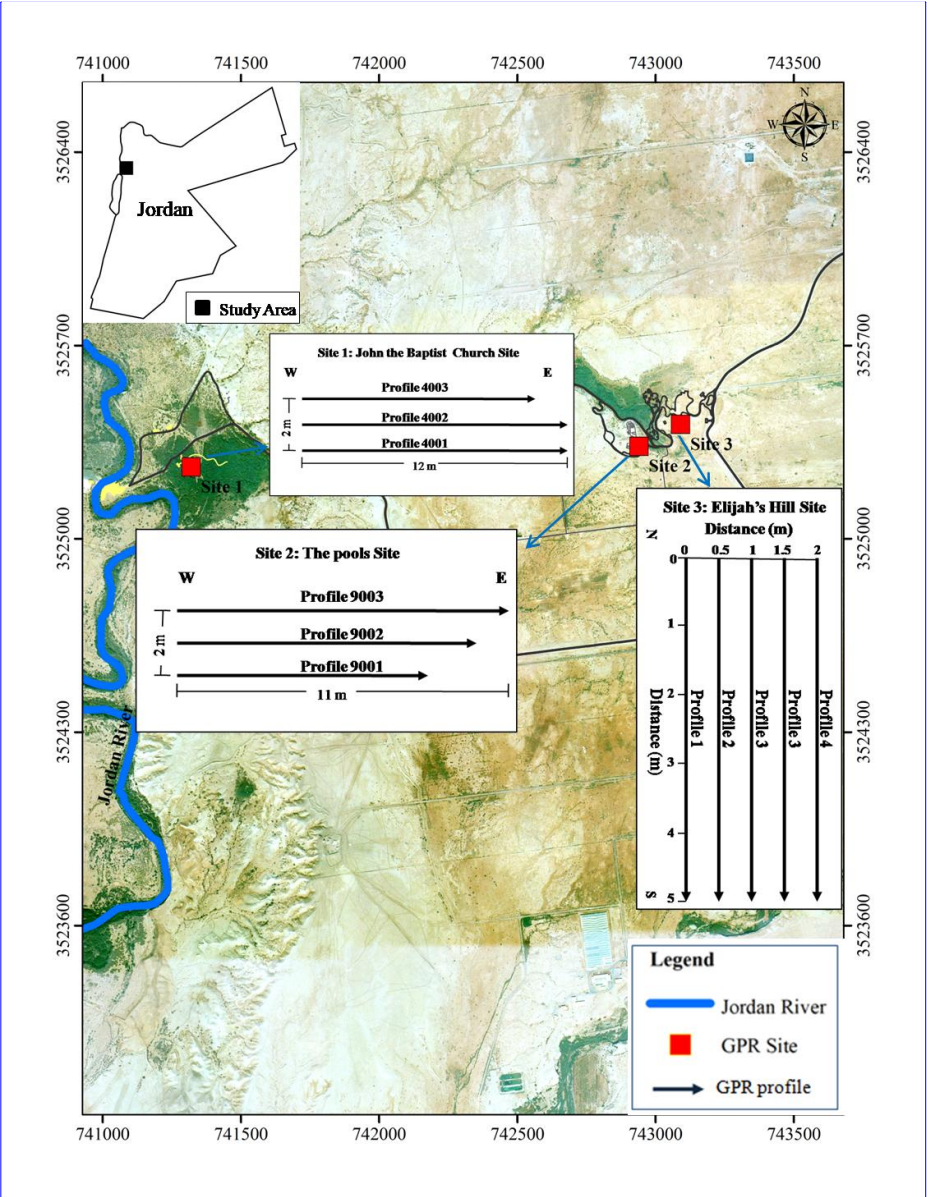
248 The authors would thank the Ministry of high education and scientific research for their
249 fund and support throughout the project. We would also like to thank Eng. B. El-Madani,
250 the former Baptism site Commission Director and his assistant Eng R. Mkhjian for their
251 help. We are also grateful to the technicians, I. Aldabas, M. Aqrabawi, Z. Heyassat the
252 employees of (BAU) for their efforts during data acquisition in the fieldwork. We thank
253 the anonymous reviewers and the editor for their constructive critics and comments on
254 this manuscript very much.

255 **References**

256 Abueladas, A.: Ground Penetrating Radar Investigations of Active Faults and Antiquities
257 along the
258 Dead Sea Transform in Aqaba and Taba Sabkha, Jordan, master thesis, University of
259 Missouri-Kansas City, U.S.A, 71 pp., 2005.
260 Annan, AP.: GPR principles, procedures and applications: Sensors and Software In,
261 2003.
262 Aqeel, A., Anderson, N., and Maerz, N.: Mapping sub-vertical discontinuities in rock
263 cuts using a 400-
264 MHz ground penetrating radar antenna, Arab J Geosci 7(5), 2093–2105,
265 <https://doi.org/10.1007/s12517-013-0937-y>, 2014.
266 Basile, L., Carrozzo, MT, Negri, S., Nuzzo, S., Quarta, L., and Villani, A.V.: A ground-
267 penetrating radar survey for Archaeological investigations in an urban area (Lecce, Italy),
268 Journal of Applied Geophysics, 44, 15-32, [https://doi.org/10.1016/S0926-](https://doi.org/10.1016/S0926-9851(99)00070-1)
269 [9851\(99\)00070-1](https://doi.org/10.1016/S0926-9851(99)00070-1), 2000.
270 Cacione, JM.: Radar simulation for archaeological applications: Geophysical
271 Prospecting, 44, 871-888,
272 <https://doi.org/10.1111/j.1365-2478.1996.tb00178.x>, 1996.
273 Eppelbaum, L.V., and Khesin, B.E.: Disturbing factors in geophysical investigations at
274 archaeological sites
275 and ways of their elimination. In: Transactions of the IV Conference on Archaeological
276 Propection, Vienna, Austria, 19-23 September 2001, 99–10, 2001
277 Eppelbaum, L.V., Khesin, B.E. and Itkis, S.E.: Archaeological geophysics in arid
278 environments: Examples from Israel, Journal of Arid Environments, 74, 849-860,
279 <https://doi.org/10.1016/j.jaridenv.2009.04.018>, 2010.
280 Gracia, V., Garcı, F., Pujades, L., Drigo, R., and Capua, D.: GPR survey to study the
281 restoration of a Roman monument, Journal of Cultural Heritage, 9, 89-96,
282 <https://doi.org/10.1016/j.culher.2007.09.003>, , 2008.
283 Fisher, E.: Examples of reverse-time migration of single-channel, ground penetrating
284 radar profiles. Geophysics, 57, 577-586, <https://doi.org/10.1190/1.1443271>, 2006.

285 Knapp, R. W.: Vertical resolution of thick beds, thin beds and thin-bed cyclothem,
286 Geophysics, 55, 1183-119, <https://doi.org/10.1190/1.1442934>, 1990.
287 Neal, A.: Ground-penetrating radar and its use in sedimentology: principles, problems
288 and progress, Earth-Science Reviews, 6, 261–330,
289 <https://doi.org/10.1016/j.earscirev.2004.01.004>, 2004.
290 Odah, H., Ismail, A., Elhemaly, I., Anderson, N., Abbas, A., and Shaaban, F.:
291 Archaeological exploration using magnetic and GPR methods at the first court of
292 Hatshepsut Temple in Luxor, Egypt, Arab J. Geosci., 6, 865–871,
293 <https://doi.org/10.1007/s12517-011-0380-x>, 2014.
294 Ronen A, Ezersky M, Beck A., Gat enio B., Simhayov R.B (2018) Use of GPR method
295 for prediction of sinkholes formation along the Dead Sea Shores, Israel. Geomorphology
296 328: 28-43.
297 <https://doi.org/10.1016/j.geomorph.2018.11.030>
298 Sheriff, R. E., and Geldart, L. P.: Reflection field methods, Cambridge University Press,
299 England, 1995.
300 Sternberg, B. K., McGill, J. W.: Archaeology studies in southern Arizona using ground
301 penetrating radar. Journal of Applied Geophysics, 33, 209-225,
302 [https://doi.org/10.1016/0926-9851\(95\)90042-X](https://doi.org/10.1016/0926-9851(95)90042-X), 1995.
303 Vaughan C. J.: Ground penetrating radar survey used in archaeological investigations.
304 Geophysics, 51, 595-604, <https://doi.org/10.1190/1.1442114>., 1986.
305 Waheeb, M (2003) Recent Discoveries in the Bethany Beyond Jordan in Jordan Valley.
306 ADAJ 47:243-246.
307 Waheeb M (2001) Archaeological Excavations at the Baptism Site, Bethany Beyond the
308 Jordan. Bible and Spade 14(2):43-53.
309 Whiting, B, McFarland, D., and Hackenberger, S.: Three-Dimensional GPR study of a
310 prehistoric site in Barbados, West Indies. Journal of Applied Geophysics, 47, 217-226,
311 [https://doi.org/10.1016/S0926-9851\(01\)00066-0](https://doi.org/10.1016/S0926-9851(01)00066-0), 2001.
312

Comment [EA1]: A colored figures



313
314
315

Figure-1

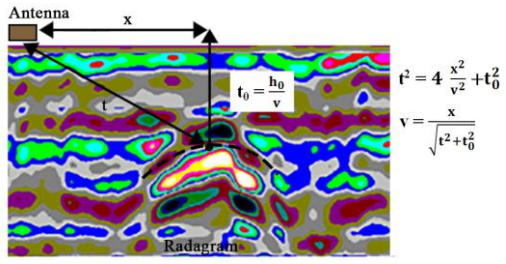


Figure-2

316
 317
 318
 319
 320
 321
 322
 323
 324
 325
 326
 327
 328
 329
 330
 331
 332
 333
 334
 335
 336
 337
 338
 339
 340
 341
 342
 343
 344

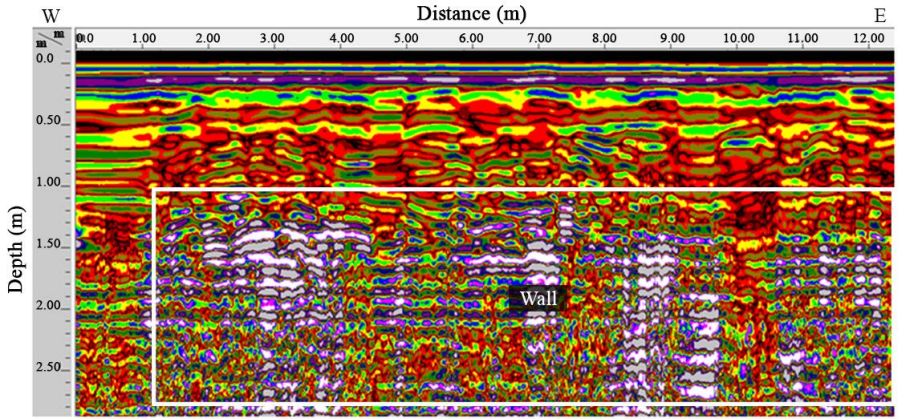
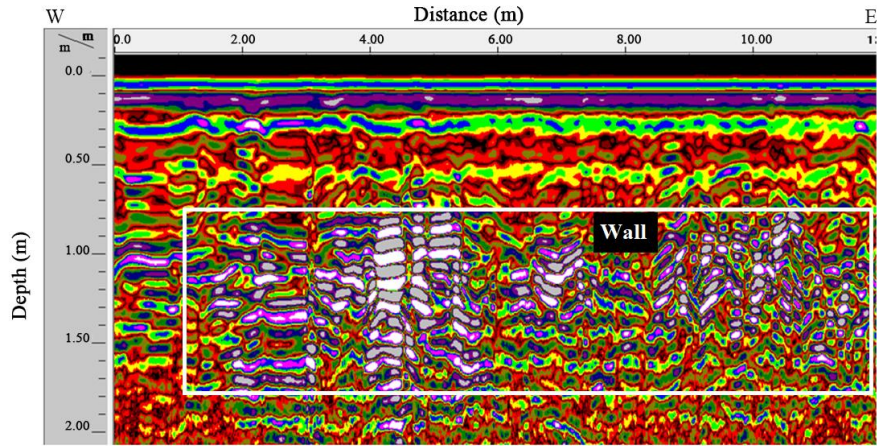


Figure-3

345
346
347
348
349
350
351
352
353
354
355
356
357
358
359
360
361
362
363
364
365
366
367
368
369
370
371
372
373
374
375
376
377



378
379
380
381
382
383
384
385
386
387
388
389
390
391
392
393
394
395
396
397
398
399
400
401
402
403
404
405
406
407
408

Figure-4

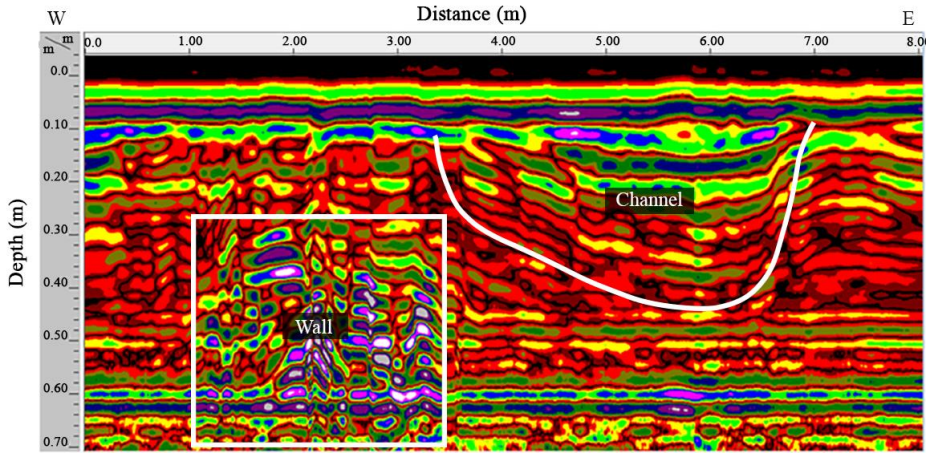
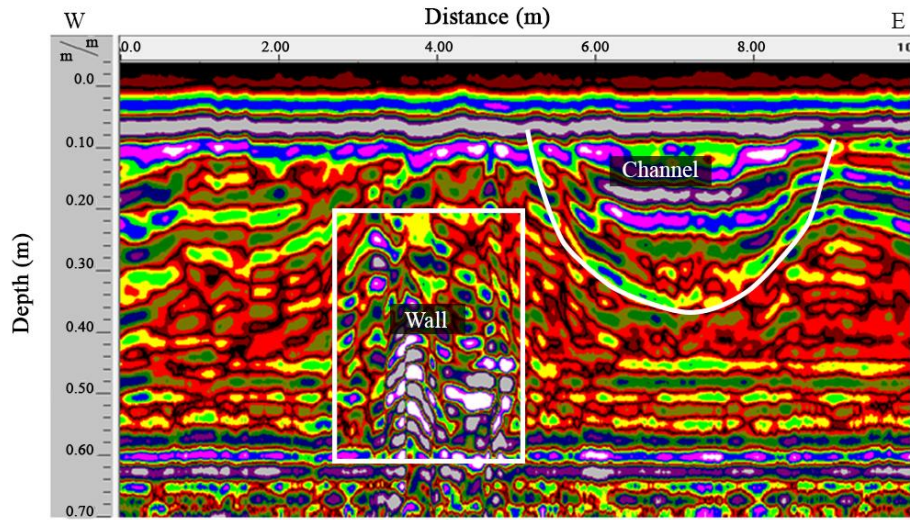


Figure-5

409
410
411
412
413
414
415
416
417
418
419
420
421
422
423
424
425
426
427
428
429
430
431
432
433
434
435
436
437



438
 439
 440
 441
 442
 443
 444
 445
 446
 447
 448
 449
 450
 451
 452
 453
 454
 455
 456
 457
 458
 459

Figure-6

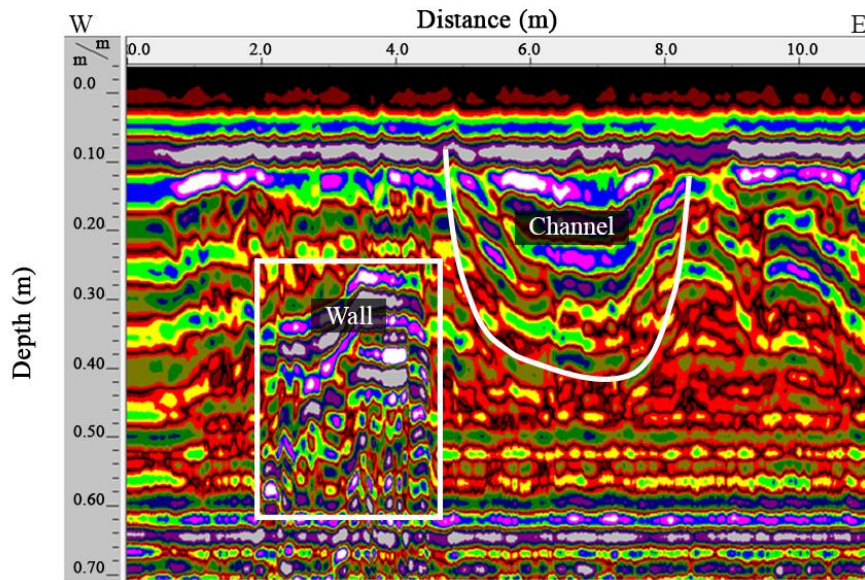
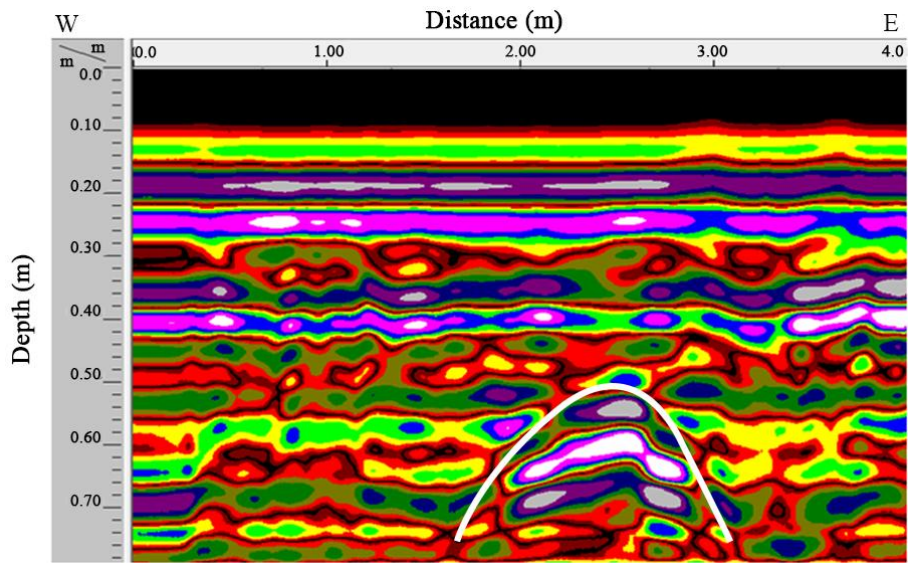


Figure-7

460
 461
 462
 463
 464
 465
 466
 467
 468
 469
 470
 471
 472
 473
 474
 475
 476
 477
 478
 479
 480
 481
 482
 483
 484
 485
 486



487
488
489
490
491
492
493
494
495
496
497
498
499
500
501
502
503
504
505
506
507
508
509
510
511
512
513
514

Figure-8

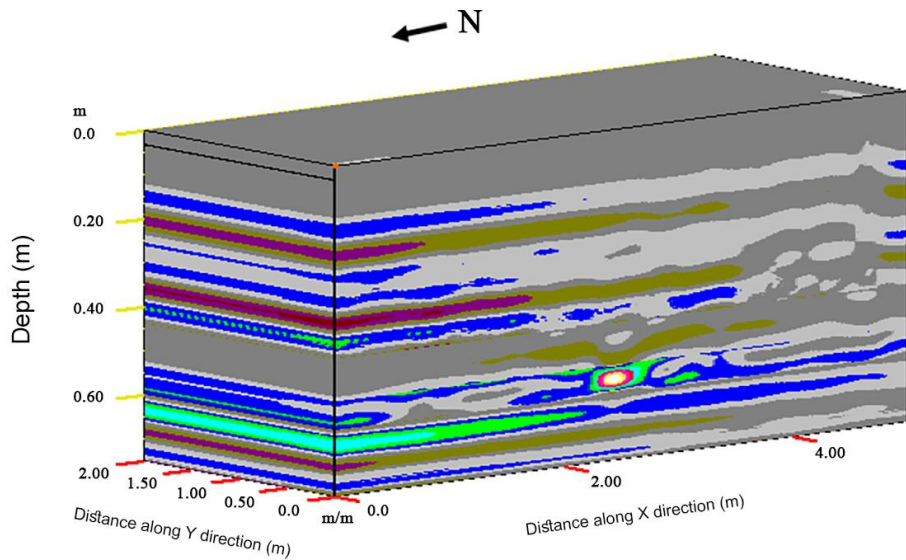


Figure-9

515
 516
 517
 518
 519
 520
 521
 522
 523
 524
 525
 526
 527
 528
 529
 530
 531
 532
 533
 534
 535
 536
 537
 538
 539
 540

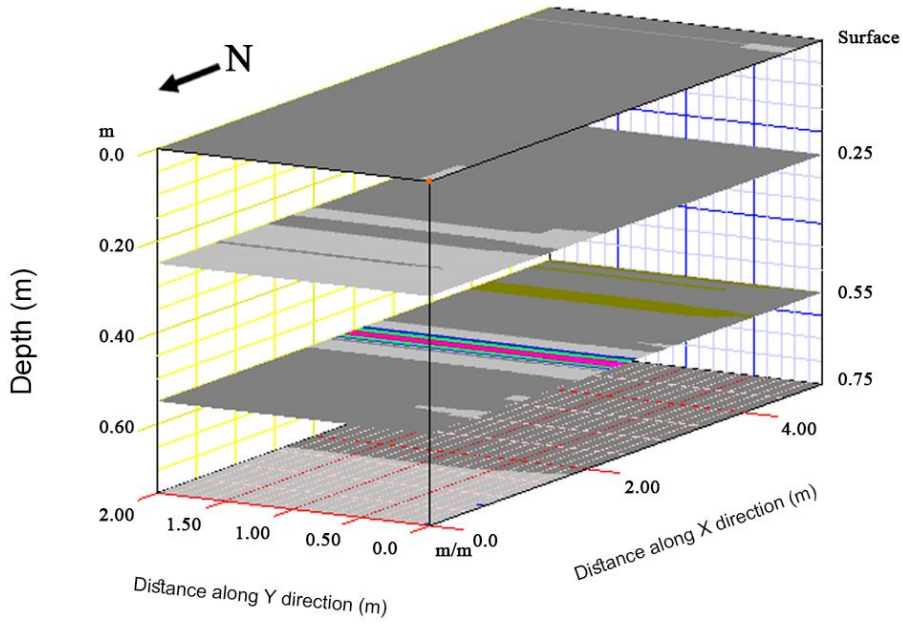
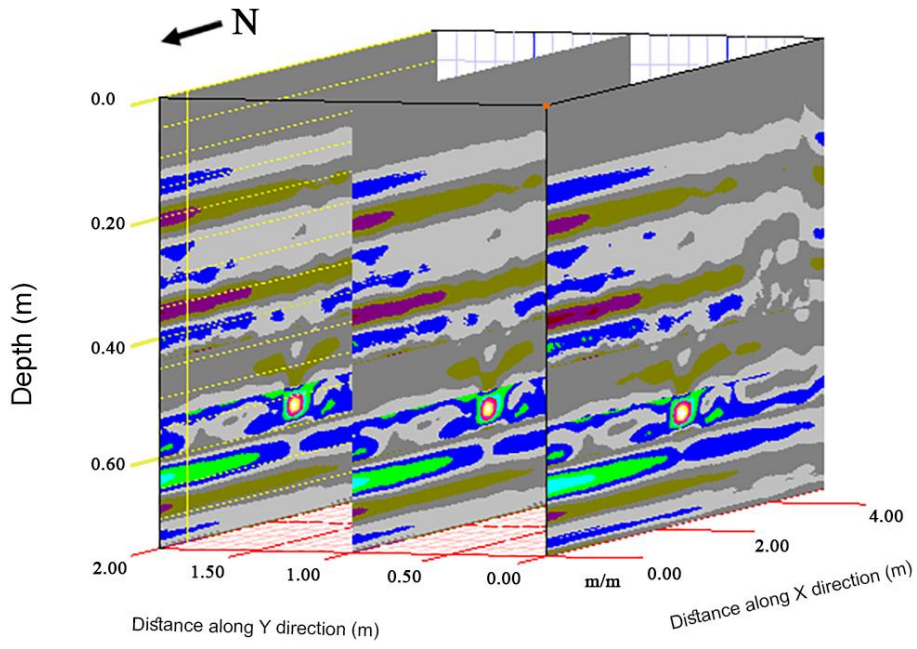


Figure-10

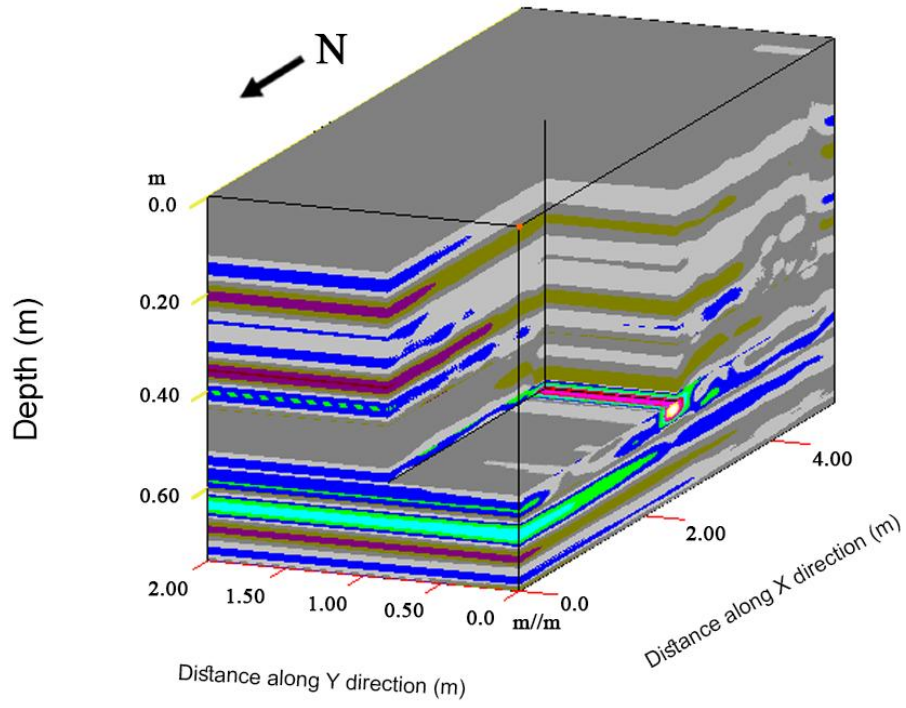
541
 542
 543
 544
 545
 546
 547
 548
 549
 550
 551
 552
 553
 554
 555
 556
 557
 558
 559
 560
 561
 562
 563
 564
 565
 566
 567
 568
 569
 570

571

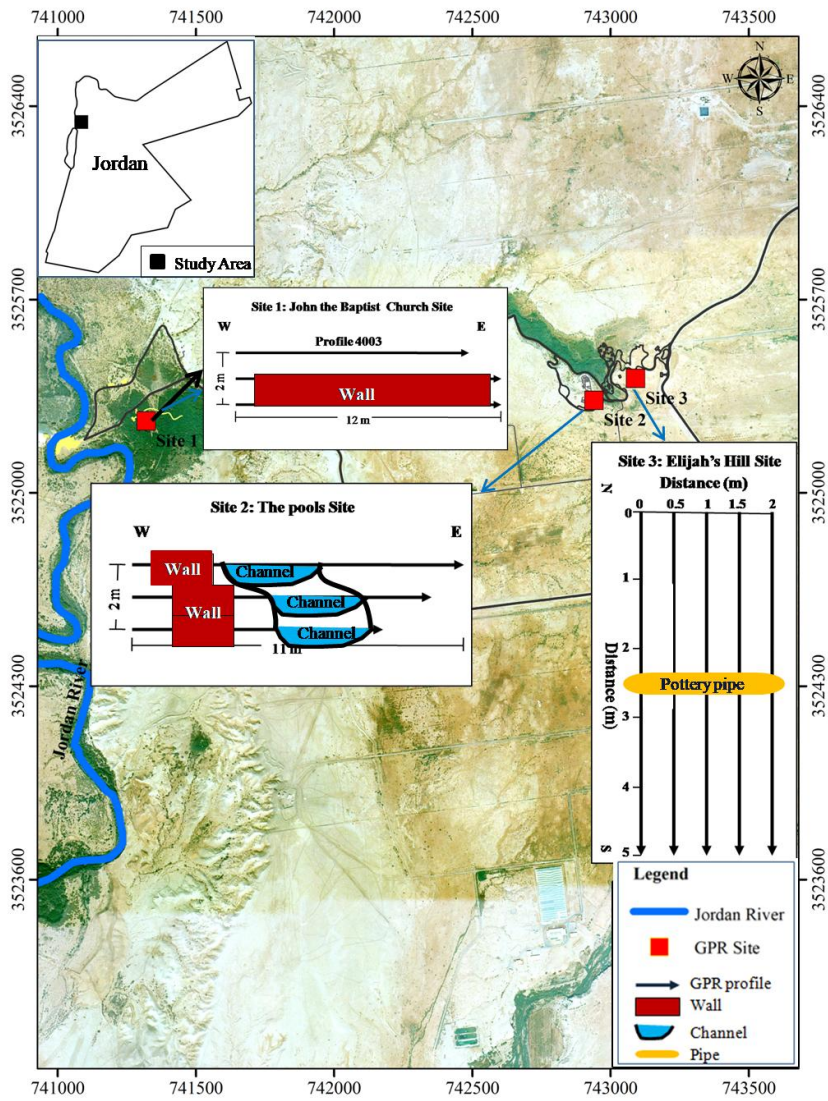


572
573
574
575

Figure-11



576
 577 **Figure-12**



578

579 Figure-13

580

581

582 **Figures Captures**

583 Fig.1. Location map of the GPR profiles study area (After Google Earth).

584 Fig.2. Hyperbolic reflections caused by pottery pipe is used to obtain the wave velocity with the equation of
585 hyperbola.
586 Fig.3. A 400 MHz antenna radargram along Profile4001. The white rectangle along the radargram at
587 approximate depth of 1.2 m may correspond to buried wall.
588 Fig.4. A 400 MHz antenna radargram along Profile4002. The white rectangle along the radargram at
589 approximate depth of 0.6 m may correspond to buried wall.
590 Fig.5. A 900 MHz antenna radargram along Profile9001. The white rectangle along the radargram
591 represents anomaly located between horizontal distance 1 and 3 m with approximate depth 0.25 m which
592 may correspond to an ancient buried wall. The 4 m wide depression at end of the profile may be correlated
593 to buried channel.
594 Fig.6. A 900 MHz antenna radargram along Profile9002. The white rectangle along the radargram at
595 approximate depth of 0.20 m may correspond to buried wall. The 4 m wide depression at end of the profile
596 may be correlated to buried channel.
597 Fig.7. A 900 MHz antenna radargram along Profile9003. The white rectangle along the radargram at
598 approximate depth of 0.20 m may correspond to buried wall. The 4 m wide depression at end of the profile
599 may be correlated to buried channel.
600 Fig. 8 A part of 900 MHz antennae radargram along profile 1 immediately adjacent to excavated pottery
601 pipe. The hyperbolic- shaped anomaly at distance 2.5 m and 0.55 m deep shows the extension location of
602 the buried pottery pipe.
603 Fig. 9 The 3D GPR data view constructed from 2D profile lines. The 3D perspective view of processed
604 profiles using high pass and low pass vertical and horizontal filters together with migration technique that
605 show the location of the pottery pipe.
606 Fig.10. Depth slices with different depths (0, 0.25, 0.55, 0.75 m) generated from 3D plot . The main
607 anomaly observed with W-E direction at depth slice 0.55 mbs (meter below surface).
608 Fig.11. The multiple slices view along y direction at distance (0, 1 and 2 m) determines the depth and
609 extension of the pipe.
610 Fig.12. The 3D section (cutout cube) using X=2.5 m, Y=0.85 m, and Z=0.55 m shows clearly the depth and
611 extension of the pipe perpendicular to the X position and the depth of the top of pipe detect by the Z
612 position.
613 Fig.13. Location map of the inferred archaeological material (after Google Earth)
614
615